

Post-Disruptive Runaway Electron Beam in COMPASS Tokamak

Milos VLAINIC^{1,2†}, J. MLYNAR², J. CAVALIER²,
V. WEINZETTL², R. PAPROK^{2,3}, M. IMRISEK²³⁴,
O. FICKER^{2,4}, J.-M. NOTERDAEME^{1,5}
AND the COMPASS Team

¹Department of Applied Physics, Ghent University, Ghent B9000, Belgium

²Institute of Plasma Physics AS CR, Prague 18200, Czech Republic

³Faculty of Mathematics and Physics, Charles University, Prague 12116, Czech Republic

⁴Faculty of Nuclear Sciences and Physical Engineering, Czech Technical University, Prague 11519, Czech Republic

⁵Max Planck Institute for Plasma Physics, Garching D-85748, Germany

(Received ?; revised ?; accepted ?. - To be entered by editorial office)

For ITER-relevant runaway electron studies, such as suppression, mitigation, termination and/or control of runaway beam, obtaining the runaway electrons after the disruption is important. In this paper we report on the first achieved discharges with post-disruptive runaway electron beam, entitled “runaway plateau”, in the COMPASS tokamak. The runaway plateau is produced by massive gas injection of argon. Almost all of the disruptions with runaway electron plateaus occurred during the plasma current ramp-up phase. Comparison between the Ar injection discharges with and without plateau has been done for various parameters. Parametrisation of the discharges shows that COMPASS disruptions fulfill the range of parameters important for the runaway plateau occurrence. These parameters include electron density, electric field, disruption speed, effective safety factor, maximum current quench electric field. In addition to these typical parameters, the plasma current value just before the massive gas injection surprisingly proved to be important.

1. Introduction

As the tokamak concept developed in the last 50 years and advanced towards the ITER design, numerous challenges occurred and many were solved. One of the remaining tasks is control or mitigation of Runaway Electrons (RE) in ITER after the disruption. Estimations from codes predict RE with several tens of MeV to carry up to 70% of pre-disruptive plasma current (Hender *et al.* 2007, p. S178). As deposition of runaway electron beam can be highly localised, it could severely damage plasma facing components and blanket modules of ITER.

The electron is said to run away, when the collisional drag force acting on it becomes smaller than the accelerating force coming from the toroidal electric field E_{tor} . There are three main mechanisms for the runaway generation: a) Dreicer (primary) mechanism (Dreicer 1959, 1960); b) hot-tail mechanism (Smith & Verwichte 2008); c) avalanche (secondary) mechanism (Rosenbluth & Putvinski 1997). However, there is a theoretical limit for the electrical field, so called critical field E_{crit} , under which RE cannot be produced by these mechanisms (Connor & Hastie 1975). The toroidal electric field E_{tor} in

† Email address for correspondence: milos.vlainic@ugent.be

ITER during the stable discharge will be under the E_{crit} threshold, making the controlled ITER plasma void of the RE. On the other hand, if disruption occurs, the electron temperature T_e would drop during Thermal Quench (TQ), and thus plasma electric resistivity η would increase. E_{tor} , being proportional to ηj , will rise dramatically during the Current Quench (CQ), because the current density j drops much slower than the electric resistivity increase due to the vessel electromagnetic field penetration time. This increase of the field will first induce runaway seeds that will then be multiplied enormously by the avalanche effect. In the ITER disruption scenarios, the avalanche multiplication factor could be as large as 10^{22} (Hender *et al.* 2007, table 5), forming an electron beam that could threaten ITER's first wall structure. Following the above outline, ITER should be equipped with a proper suppression and/or mitigation technique dedicated to the RE control. Thus, achieving post-disruptive RE beam is one of the first significant steps for COMPASS towards the ITER-relevant runaway suppression/mitigation studies.

The COMPASS tokamak (Pánek *et al.* 2006) is a small-size experimental fusion device with major radius $R_0 = 0.56$ cm and minor radius $a = 0.23$ cm. Toroidal magnetic field B_{tor} is in $0.9 - 1.25$ T range and plasma current I_p can reach up to 330 kA. Electron densities are flexible and are typically of order of magnitude of $10^{19} - 10^{20}$ m $^{-3}$. Plasma shaping varies from circular and elliptical to single-null D-shaped ITER-like plasmas. The typical pulse length is 0.4 s, although the low current circular discharge with RE can last almost 1 s. Furthermore, flexibility of various plasma parameters (e.g. shaping, densities, plasma current, etc.) combined with significant, but still safe, runaway population make COMPASS suitable for runaway models validation and scaling towards ITER.

In contrary to large tokamaks (e.g. JET, ITER), where most of the RE are produced during the disruption (Martin *et al.* 1995; Yoshino *et al.* 1999; Gill *et al.* 2000), in small and medium size tokamaks RE are created either during the current ramp-up or the flat-top phase (Esposito *et al.* 2003; Papřok *et al.* 2013) when n_e is low and/or E_{tor} is high enough. Additionally, the present COMPASS maximum value for B_{tor} is 1.25 T, while various observations noted that getting the post-disruptive RE spontaneously is not possible if B_{tor} is under ≈ 2 T (Martin *et al.* 1995; Yoshino *et al.* 1999; Gill *et al.* 2002). The B_{tor} -limit is the most probable reason for the lack of post-disruptive runaway observations in COMPASS. Therefore, size of the COMPASS and its maximum B_{tor} could discard this facility from the ITER-relevant runaway suppression/mitigation research. Nevertheless, some of optimism can be found in experiments in which the post-disruptive RE were achieved with high-Z Massive Gas Injection (MGI) (Yoshino *et al.* 1999; Gill *et al.* 2002; Hollmann *et al.* 2013) or high-Z pellet injection (Yoshino *et al.* 1999; Hollmann *et al.* 2013), since some of these experiments had B_{tor} lower than 2 T. Moreover, a detailed study of B_{tor} -limit as a function of amount of Ar injected was performed recently in JET (Reux *et al.* 2014), where post-disruptive RE were observed even for $B_{tor} = 1.2$ T. Therefore, Ar injection was used to trigger the first post-disruptive RE in COMPASS.

The paper is organised as follows: in section 2, the experimental setup used for the experiments and demonstration of runaway plateau observation is presented. In section 3, general runaway parameters are reported, followed by the injection and disruption details. The section is finalised with the discharge analyses of the parameters important for the plateau occurrence. In section 4, the results presented in section 3 are discussed. Finally, in section 5 conclusions and future perspectives are addressed.

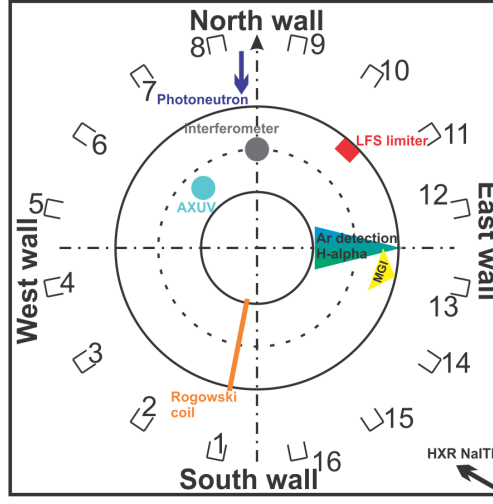


Figure 1: Principal diagnostics used for the RE plateau studies.

2. Introduction to Experiment

2.1. Experimental Setup

In all discharges described in this paper the plasmas were circular - limited by the carbon High Field Side (HFS) wall - with additional carbon Low Field Side (LFS) limiter for the inner wall vessel protection (see Fig. 1). Typical magnetic field B_{tor} was 1.15 T and plasma currents I_p at the moment of the gas injection varied from 40 to 140 kA. The electron density n_e was relatively low ($0.8 - 2.2 \times 10^{19} \text{ m}^{-3}$) for maximising the runaway generation. Schematics of the experimental setup used in the experiments presented in this article is shown in Fig. 1. In this article, measurements of runaway losses will be presented from PhotoNeutron (PN) detector located nearby the north wall and NaI(Tl) scintillator for Hard X-Ray (HXR) detection located at the south-east part of the tokamak hall. Both detectors are approximately 5 m from the vessel. Photoneutrons with energy of few MeV are observed with the ZnS(Ag) neutron detector embedded in a plastic matrix. Beside the neutrons, the PN detector is suspected to be sensitive to the strong fluxes of HXR, although the detector is shielded by 10 cm of Pb. HXR are measured with unshielded NaI(Tl) scintillation detector, where the signal is amplified with a photomultiplier tube and the energy range is approximately from 100 keV to few MeV. Furthermore, the low energy photon radiation measurements will be presented from H_α detector and the bolometry. H_α detector is located radially at the east part of the tokamak vessel. AXUV photodiodes, located at the north-west part of the tokamak vessel, with photon energy response from 7 eV to 10 keV are used for bolometric measurements.

MGI of argon was achieved using a solenoid valve, located on the east side of the tokamak. The solenoid gas valve is connected to the vessel through two stainless steel tubes: the first one is 20 cm long and has an inner diameter of 4 mm, while the second one is 40 cm long and has an inner diameter of 6 mm. This non-negligible tube length implies a delay between the time of valve opening and the time at which the argon puff starts to interact with the plasma, i.e. roughly the time at which the gas enters the vacuum vessel. The delay is estimated to be approximately 1 ms taking into account a mean velocity of approximately 400 m/s for argon gas in vacuum at 300 K.

The Ar flow rate dN/dt through the injection system was evaluated experimentally as a function of the back pressure p_{back} and with linear dependence as follows:

$$\frac{dN}{dt} = (9.5511 p_{back} - 1.0083) 10^{20}, \quad (2.1)$$

where p_{back} is in bars and dN/dt is in particles/s. The pressure p_{back} used for the plateau discharges were 2.4 and 1.2 bar, corresponding to particle flow rates of 2×10^{21} and 10^{21} particles/s, respectively. The valve is roughly estimated to be open 2 ms, better knowlegde of gas valve performance will be available soon by the installation of a fast opening and more reliable valve.

Since there is a pipe between the valve and the tokamak vessel, the duration time for Ar to enter the vessel is larger then the opening time of the valve and this Ar puff duration in the tokamak vessel will be estimated here. For the two aforementioned back pressures, 2.4 bar and 1.2 bar, the manufacturer gives a flux through the solenoid valve at standard conditions of 100 and 50 Pa m³/s corresponding to flow rates of 2.4×10^{22} and 1.2×10^{22} particles/s at 300 K, respectively. Therefore, assuming a constant flow rate of the solenoid gas valve with the increase of pressure in the stainless steel pipe and neglecting the flow rate through the injection system in the tokamak, one can calculate the number of particles that fill the pipe and that will be puffed in the tokamak later on. Remembering that the valve stays open for about 2 ms, one can find that there will be about 5×10^{19} and 2.5×10^{19} particles for 2.4 bar and 1.2 bar, respectively. Notice that these numbers are much smaller than the total number of particles that can be stored in the pipes at 2.4 bar and 1.2 bar (8×10^{22} and 4×10^{22} respectively), justifying the assumption of constant flow rate through the solenoid valve. Now, knowing the flow rate through the injection system and the number of particles in the pipes, one can give an estimation of what the Ar puff duration in the tokamak vessel is: 25 ms for 2.4 bar and 12.5 ms for 1.2 bar. The runaway plateau created in this manner lasted from 2.5 to 10 ms.

2.2. Plateau Observation

An example of a typical COMPASS discharge with MGI generated runaway plateau is shown in Fig. 2a, together with slow I_p decay for comparison in Fig. 2b. Fig. 2a shows the plateau discharge #8585, when Ar puff starts to cool down the plasma, I_p starts to drop and plasma radiation increases. After approximately 2 ms (this delay will be justified in the next section), TQ occurs and almost all plasma energy is radiated. At the same time the HXR measurement shows relatively low peaks in half saturated state and PN signal is rather low, meaning that high energy RE created during the discharge initial phase are still confined. Then, during the CQ, E_{tor} is increased and boosts runaway production creating and amplifying the runaway beam. After the CQ the runaway beam carries non-zero current called I_{RE} , lasting for few milliseconds as one can see from the top graph in Fig. 2a. Finally, the RE beam terminates with the loss seen in HXR and PN signals, while there are almost no H_α radiation and radiated power P_{rad} from plasma proving the runaway plateau existence. On the other hand, the COMPASS discharge #8668 (see Fig. 2b) displays an example of the slow radiative decay with MGI on COMPASS resembling to I_p ramp-down, for which no TQ and CQ (a typical sign of fast disruption) are observed. In this discharge plasma radiates on a long time scale (≈ 20 ms). Although HXR and PN signals show presence of released RE, we shall not consider this as the runaway plateau, because the I_p current is mainly driven by the thermalised plasma and not by the runaway beam, as one can see from strong H_α emission. Notice that the difference in H_α and P_{rad} measurements makes the distinction between the runaway plateau and the slow radiative I_p decay. The former one has a relatively low radiation

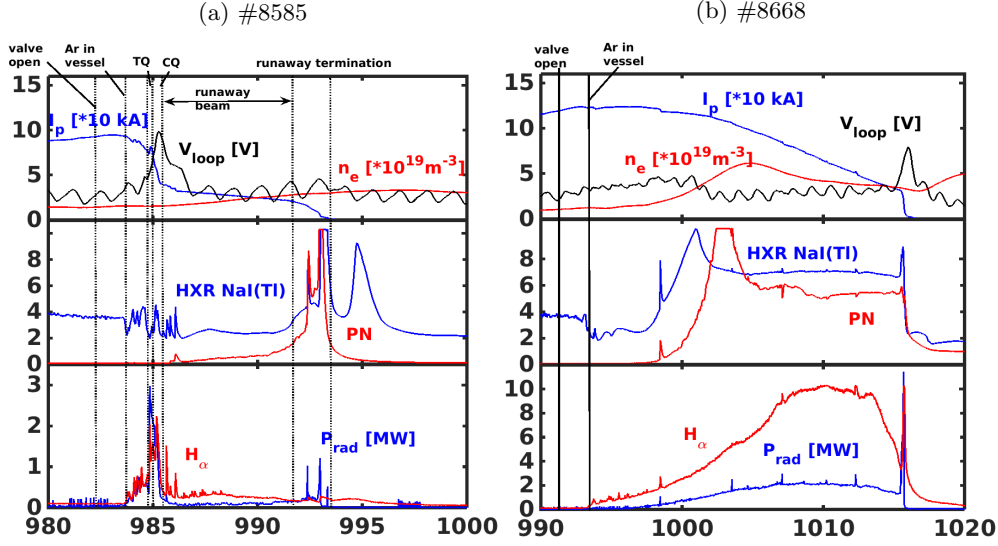


Figure 2: Time evolution of the COMPASS discharge #8585 as an example for runaway beam (a) and #8668 as an example for slow I_p decay (b) both initiated by the MGI. Plasma current I_p , electron density n_e and loop voltage V_{loop} are plotted on the top, in the middle HXR and PN signals are showing RE losses on the wall, while the H_α and P_{rad} measurements are showing the radiation losses from plasma on the bottom (N.B. The y-axis are different for the bottom plot of the two discharges).

level after the disruption, indicating that there is only cold plasma beside the runaway population.

Supplementary to the previous description of the RE plateau, the observation of RE beam with visible camera is displayed in Fig.3 for discharge #8585. The creation and localisation of the beam are well visible.

3. Results

Out of 137 discharges performed during the COMPASS RE campaign, Ar puff was used in 39 discharges where only 5 discharges ended in spontaneous disruption. Out of the 39 discharges, 14 had the RE plateau after the Ar puff, while 9 resulted in slow radiative I_p decay, similar to a ramp-down. The remaining 11 discharges ended in a typical COMPASS disruption, i.e. without any RE.

Based on these observations, all discharges with the Ar puff can be classified as:

- (a) STRONG (RE plateau) - $I_{RE} > 5$ kA
- (b) WEAK (RE plateau) - $I_{RE} < 5$ kA
- (c) SLOW (radiative current decay) - plasma current slowly decreases in the similar manner as a ramp-down phase
- (d) ZERO (RE plateau) - “typical” disruption for COMPASS with no RE remaining or generated after the disruption

An example of each class is shown in Fig. 4, where Fig. 4b is a zoom of Fig. 4a to emphasize the difference between weak and zero plateau measurements. Although these two cases could seem identical at the first sight, the PN signal confirms release of the RE after the disruption in the weak case (b) and their loss during the disruption in the zero

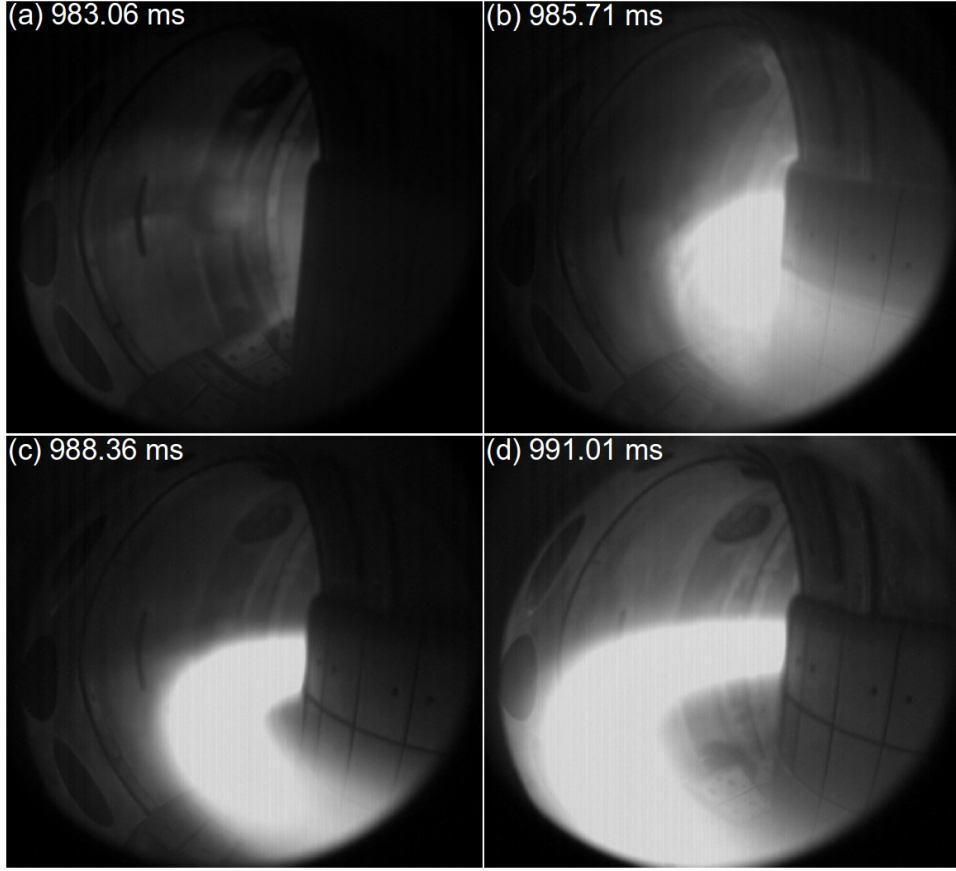


Figure 3: Visual observation of the RE beam with visible camera for discharge #8585: (a) before Ar reaches vessel, (b) formation of the RE beam on HFS, (c) RE beam and (d) RE beam drifts towards LFS.

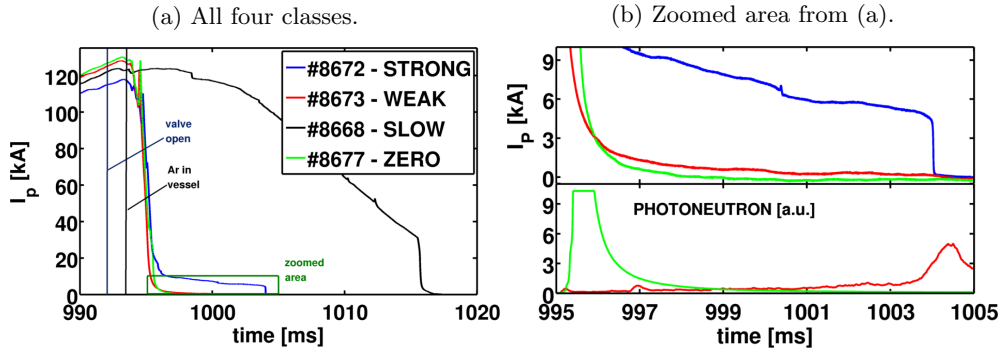


Figure 4: Classification examples: (a) #8672 for strong plateau, #8673 for weak plateau, #8668 for slow plasma current decay and #8677 as an example of disruption without RE surviving or produced; (b) Zoomed region from part (a) for better observation of the difference between weak and zero plateau, as well as photoneutron signal for comparison of weak and zeros cases.

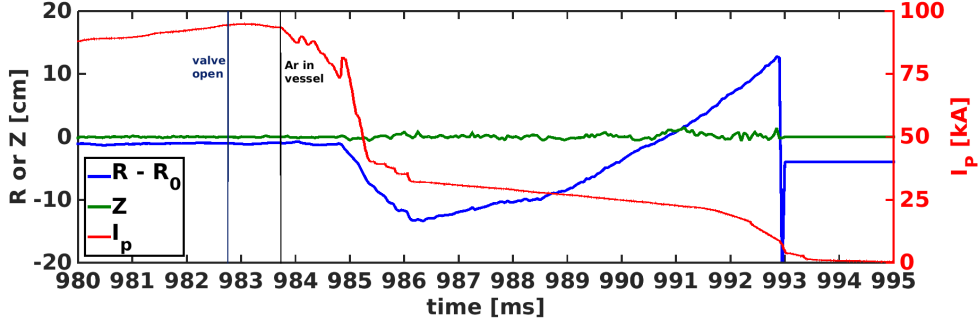


Figure 5: Time evolution of plasma vertical Z and horizontal $R - R_0$ positions for the COMPASS discharge #8585, associated with the plasma current I_p barycentre. Positive values of $R - R_0$ mean that the plasma I_p barycenter is closer to the LFS and positive values of Z mean that the plasma I_p barycentre is closer to the top of the vessel.

case (d). This classification is very important, as it will be used from now on throughout the paper. We shall now present the main results of the RE COMPASS campaign.

First, we have estimated the typical maximum runaway energy for the analyzed discharges to be 10–15 MeV by taking into account the electron acceleration due to electric field with the synchrotron radiation losses only, as suggested in Martín-Solís *et al.* (2010); Yu *et al.* (2013).

Second, since the RE before or during the disruption are more likely to be produced in the hottest center of the plasma (Gill *et al.* 2002), the remaining and newly produced post-disruptive RE may have more peaked radial current profile than the pre-disruption I_p profile. The peaking represents localisation of the plasma current I_p around the magnetic axis and can be expressed through the internal inductance l_i , which is calculated by the EFIT reconstruction (Havlíček & Hronová 2010) at COMPASS. It was observed that the l_i value increases by only 5-45% in comparison to measurements on JET (Loarte *et al.* 2011). In addition to the modest l_i rise, the normalised plasma pressure β_n rises above 1.5 for the same discharges and thus confirms that the overestimated β_n as seen by EFIT (Vlainić *et al.* 2014) is caused by the presence of RE.

The inward motion (towards the HFS wall, negative $R - R_0$ values in Fig. 5) of the post-disruptive plasma, followed by its return towards the vessel center is in agreement with the TFTR (Fredrickson *et al.* 2015) and Tore Supra (Saint-Laurent *et al.* 2009) observations. However, TFTR and Tore Supra feedback systems were able to stabilise the runaway beam, while presently in COMPASS the beam continues to shift outwards until its termination, as shown in Fig. 5. Note that the outward shift is also visible in Fig. 3. The vertical plasma position for the majority of cases is rather stable (an example being given in Fig. 5), only in a few discharges some downward shifts were noticed.

3.1. Disruption Generated by Argon

As already mentioned, a solenoid valve was used to inject Ar gas into the plasma. Even though two different pressures were used (2.4 and 1.2 bar), no particular differences in runaway beam parameters were identified. The reason could be that the pressure was only varied by a factor of 2.

In devices larger than COMPASS, high-Z gas injection is used to trigger fast CQ in order to improve runaway generation (Reux *et al.* 2014). The plasma current quench rate

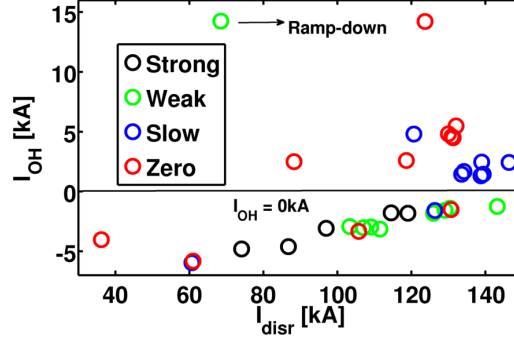


Figure 6: I_{OH} as a function of the plasma current before the gas puff I_{disr} . Negative values of I_{OH} correspond to the current ramp-up phase, while positive values represent the current flat-top and ramp-down phases.

I_γ :

$$I_\gamma = \frac{1}{I_p} \frac{dI_p}{dt} \quad (3.1)$$

is the quantifying parameter for the CQ speed. The calculation of I_γ values for disruptions with and without Ar puff was performed. No particular differences were observed between the discharges, as the majority of the I_γ values are between $500 - 2500 \text{ s}^{-1}$ in both cases. The values implicate that the whole pre-disruptive I_p is lost in $0.4 - 2 \text{ ms}$, which is the order of magnitude of the electromagnetic field penetration time of the COMPASS vacuum vessel ($\sim 0.5 \text{ ms}$).

3.2. Parametrisation of Runaway Plateau

The ohmic heating (OH) central solenoid current I_{OH} - called MFPS in (Havlíček & Hronová 2008) - will be used to indicate on the appearance time of the runaway plateau. For the RE discharges analyzed in the article I_{OH} is negative during the current ramp-up phase followed by I_{OH} at zero value for few milliseconds during the transition towards the current flat-top phase. For the rest of the discharge, i.e. current flat-top and ramp-down, it becomes positive and controlled by the feedback system (Janky *et al.* 2014). In Fig. 6, I_{OH} 2 ms before TQ is plotted versus I_p also taken 2 ms before the TQ and denoted as I_{disr} . The reason why exactly 2 ms are taken will be seen later in this section, but it can be explained as the time before Ar starts to cool down the plasma, displayed in Fig. 4a. Also, later in the article, the measured parameters denoted with the index *disr* (e.g. E_{disr} and n_{disr}) are taken at the same time.

Fig. 6 shows that only one weak plateau out of 14 plateau discharges did not appear during the ramp-up phase, but during the ramp-down phase. Hence, RE plateaus are more likely to be produced during the current ramp-up phase than during the flat-top. The ramp-down case requires further investigation in future experiments, as only one such discharge was observed.

Yoshino *et al.* (1999) did the first detailed parametrisation of disruptions with runaway occurrence in JT-60U tokamak. According to his article, study of I_γ versus q_{eff} is important for the plateau occurrence, where the effective edge safety factor q_{eff} for circular plasma is defined as:

$$q_{eff} = \frac{5a^2 B_{tor}}{RI_p} \left[1 + \left(\frac{a}{R} \right)^2 \left(1 + \frac{(\beta_p + l_i/2)^2}{2} \right) \right]. \quad (3.2)$$

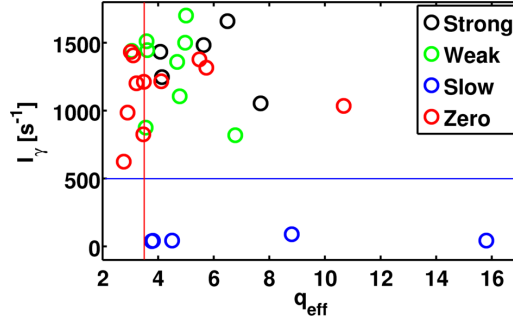


Figure 7: Plasma current quench rate I_γ as function of q_{eff} . Vertical red line corresponds to $q_{eff} = 3.5$ and horizontal blue line corresponds to $I_\gamma = 500 \text{ s}^{-1}$.

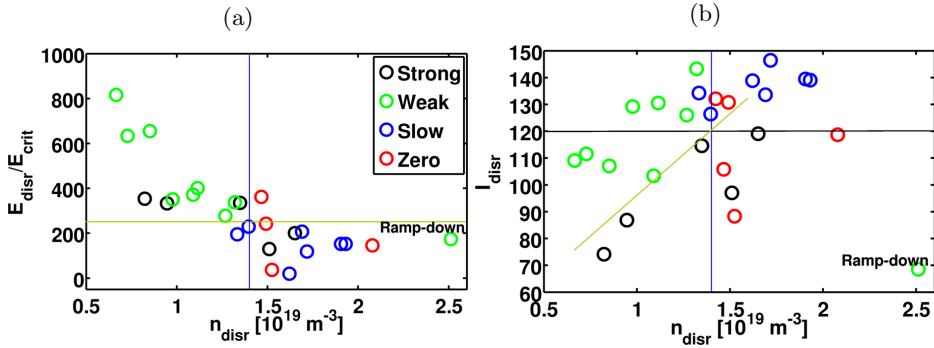


Figure 8: Normalised electric field E_{disr}/E_{crit} (a) and plasma current just before the MGI puff I_{disr} (b) as function of the electron density n_{disr} . The vertical blue line matches $n_{disr} = 1.4 \times 10^{19} \text{ m}^{-3}$. The horizontal red line in (a) corresponds to $E_{disr}/E_{crit} = 250$, while black line in (b) is for $I_{disr} = 120 \text{ kA}$. The oblique green line in (b) represents the limit between the strong and the weak case.

The internal inductance l_i and the poloidal beta β_p are taken from the EFIT reconstruction at the closest moment from the disruption. I_γ is already defined in Eq. 3.1. Fig. 7 shows I_γ versus q_{eff} for the case of COMPASS. For all plateaus except the slow ones, I_γ is between 500 and 1800 s^{-1} and q_{eff} is between 2.5 and 8. It is interesting to observe how majority of the zero disruptions are under $q_{eff} = 3.5$. Obviously, slow disruptions have significantly slower current decay than the rest of the discharges, their I_γ values are under 100 s^{-1} .

According to the theory the production of the RE is more intense for lower densities. Thus, E_{disr} normalised to E_{crit} and I_{disr} are plotted as a function of the line averaged density n_{disr} measured by the interferometer in Fig. 8. Approximately, the critical value of electron density for obtaining the runaway plateau seems to be $1.4 \times 10^{19} \text{ m}^{-3}$. The ratio E_{disr}/E_{crit} represents the relative strength of V_{loop} . Critical value of the E_{disr}/E_{crit} ratio on Fig. 8a is around 250 for the analyzed discharges. Figure 8b shows that the strong plateaus are created for lower I_{disr} value than weak plateaus, taking the same n_{disr} value. In addition, no strong plateau is observed above $I_{disr} = 120 \text{ kA}$, while half of the weak ones have I_{disr} above 120 kA.

Another parameter of interest is the current carried by the RE beam I_{RE} . The dependence of I_{RE} on the I_{disr} is shown in Fig. 9a, where only the ramp-up Ar MGI discharges

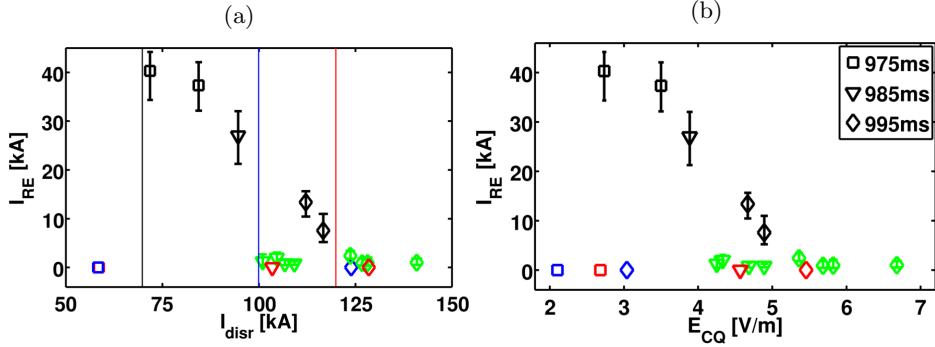


Figure 9: Runaway beam current I_{RE} as function of the pre-disruptive current I_{disr} (a) and the maximum loop voltage during the current quench E_{CQ} (b). The colors are kept the same as in previous figures, while different marker type corresponds to different times of the Ar injection: 975 ms (squares), 985 ms (triangles), 995 ms (diamonds). Symbols stand for a mean value of the I_{RE} , and error bars stand for maximum and minimum values of the I_{RE} . The vertical lines in (a) match 70 kA (black), 100 kA (blue) and 120 kA (red).

are presented. The discharges in Fig. 9 are grouped by the time of Ar puff. Typical weak plateau I_{RE} is between 0.5 – 3.5 kA, while I_{RE} for strong plateaus decreases with I_{disr} and time of the puff. Furthermore, for the Ar injections performed at 985 ms and 995 ms the upper limit of the I_{disr} is indicated, namely 100 kA and 120 kA respectively. For values lower than these I_{disr} values strong plateau seems to be produced, while above either weak plateau or no plateau occurred. In contrast to this, for the Ar injection at 975 ms the lower limit of I_{disr} is observed for about 70 kA, under which no plateau was detected. Anyway, more statistics are required. The dependence of I_{RE} on the maximum electric field E_{CQ} during the current quench (Fig. 9b) has similar behavior like in Fig. 9a, as one could expect from the self-inductance effect between I_{disr} and E_{CQ} .

4. Discussion

Even though the number of discharges devoted to runaway plateau studies was limited on COMPASS in the dedicated RE campaign, it was still possible to do comparative analyses. The results presented in the previous section are discussed in following order:

- general characteristics on RE are outlined
- observed differences between discharges with and without the runaway plateau are reported
- issues on obtaining the RE plateau with Ar puff are discussed
- achieving strong plateau is commented

In Loarte *et al.* (2011), an increase of l_i by factor of 2 to 3 has been reported for the RE plateau, which is significantly larger than the modest rise observed in COMPASS (0.05-0.45). This modest l_i rise could mean that RE seeds generated during the ramp-up phase are occurring in larger relative area than for the case of JET. Similarly to Tore Supra (Saint-Laurent *et al.* 2009), JET (Loarte *et al.* 2011) and TFTR (Fredrickson *et al.* 2015), the inward motion of the RE beam is observed for the beginning of the plateau phase at COMPASS.

Almost all (13 out of 14) generated RE plateaus were achieved for Ar puff in the ramp-up current phase, as for Tore Supra (Saint-Laurent *et al.* 2011). Regarding disruptions

itself, the CQ speed is one order of magnitude larger than for the case of JT-60U (Yoshino *et al.* 1999), where $I_\gamma > 100 - 200 \text{ s}^{-1}$ was reported as the plateau formation condition. Concluding that COMPASS has fast enough disruption for the plateau formation (see Fig. 7), but other factors - e.g. B_{tor} , V_{loop} , avalanching (Rosenbluth & Putvinski 1997) - are not fulfilled, explaining why the Ar MGI is necessary for COMPASS to obtain the runaway plateau.

Next, q_{eff} and its relation with I_γ is one more important plasma characteristics for the plateau creation. In the case of JT-60U (Yoshino *et al.* 1999), on top of the I_γ condition, q_{eff} has to be over 2.5. From Fig. 7 it is obvious that disruptions analyzed here are deep in the reported parameter region. However, there is an indication how the plateau condition for I_γ and q_{eff} in COMPASS could be different from those observed in JT-60U. Anyhow, this is still to be investigated by enhancing the statistics.

As observed from Fig. 8a, the limiting n_{disr} for plateau to appear is around $1.4 \times 10^{19} \text{ m}^{-3}$, which corresponds to $E_{crit} = 0.0122 \text{ V/m}$. The Dreicer mechanism is the most probable source of the post-disruptive production of RE at COMPASS, because the avalanching is expected to be important for the tokamaks with $I_P \gtrsim 1 \text{ MA}$ (Rosenbluth & Putvinski 1997). However, from Fig. 8a it is apparent how the strong plateaus are obtained for low E_{disr}/E_{crit} values compare to the weak plateaus. This observation, at the first sight contra-intuitive, could be explained with the appearance of the avalanching effect, as avalanching is dominant runaway generation mechanism for lower E_{disr}/E_{crit} assuming that the electron temperature profile remains unchanged (see Nilsson *et al.* 2015, Fig. 10). Anyhow, this possibility is still to be investigated. The Dreicer field E_D is currently difficult to determine as the Ar injections were often too early, so that no Thomson scattering data were collected yet. For the cases plotted in Fig. 8b, it seems that lower densities are necessary in order to achieve plateau for I_{disr} above 120 kA, making I_{disr} important parameter for the plateau production.

In the COMPASS case, it seems that the inverse dependence is recognised for the strong plateaus (Fig. 9a). The dependence of I_{RE} on I_{disr} from Fig. 9b looks almost the same as the one from Fig. 9a, as one would expect. This observation comes from the fact that the amplitude of induced E_{tor} during the CQ is directly proportional to the I_p before the disruption. Lower and upper boundary signs of plasma current for strong plateaus from Fig. 9b are not unique, these boundaries have been observed in JET by Gill *et al.* (2002). In this article, the lower limit is assigned to low E_{tor} , while the upper limit is possibly connected to magnetic fluctuations. For COMPASS more discharges would be required to improve the statistics and find the two limits.

5. Conclusion and Future Work

Before this dedicated campaign, runaway plateau was never observed in COMPASS. As a matter of fact, there was scepticism concerning the possible plateau occurrence for any plasma condition, due to the COMPASS tokamak size, low B_{tor} and the low plasma currents leading to relatively low electric field E_{tor} during the disruption. Nevertheless, in this paper a clear demonstration of obtaining runaway plateau by MGI is reported. The RE plateau currents varied between 0.5 to 40 kA, with duration from 2.5 to 10 ms.

Argon injection disrupted discharges in COMPASS have been investigated in order to clarify the necessary conditions for runaway plateau production. It was found that the easiest way to produce the RE plateau was to inject Ar during the ramp-up of the plasma current. Furthermore, the typical COMPASS disruptions without RE can satisfy various parameters important for the runaway plateau creation (e.g. n_e , V_{loop} , I_γ , q_{eff}) without Ar injection, thus high-Z MGI is probably required only for activating thermal quench

to enhance runaway population. Unusually, for the discharges considered in the paper, it seems that the plateau generation also depends on plasma current during the Ar puff injection. Even though, the CQ after MGI induced disruption has a very short time, it is possible that avalanche mechanism is present in COMPASS during the runaway plateau formation.

More experiments need to be done in order to draw final conclusions on the definite conditions for the runaway plateau generation in COMPASS tokamak. From present knowledge we can conclude that some observations correspond to reports from larger tokamaks, although the amplitude is sometimes different. Indeed, this difference in the magnitudes could be important for scaling towards ITER.

The experiment presented here confirm that COMPASS is a tokamak suitable for various ITER-relevant runaway studies, such as:

- (a) studies of runaway plateau termination - energy balances and timescales (Loarte *et al.* 2011; Martín-Solís *et al.* 2014)
- (b) improvements of the runaway beam mitigation
- (c) testing the runaway control system
- (d) benchmarking of the runaway models

Nonetheless, the scenario for inducing the runaway plateau is necessary before further ITER-relevant studies are performed. Presently, LUKE (Decker & Peysson 2004) code is being used in collaboration with CEA for a better understanding of the physics behind the measurements.

The “Joint Doctoral Programme in Nuclear Fusion Science and Engineering” is acknowledged by the first author for supporting the studies. Next to thank is the project MSMT LM2011021 from which the COMPASS operation is supported. Then, the authors would like to acknowledge work of the WP14-MST2-9 research project team. The first author would like to thank to Francois Saint-Laurent for advising and sharing his experience with us, Jozef Varju for installing the injection system and Josef Havlíček and Michael Komm for fruitful discussions. Faculty of Nuclear Sciences and Physical Engineering (Czech Technical University) is also appreciated for lending us the HXR detectors.

This work has been carried out within the framework of the EUROfusion Consortium and has received funding from the Euratom research and training programme 2014-2018 under grant agreement No 633053. The views and opinions expressed herein do not necessarily reflect those of the European Commission.

REFERENCES

- CONNOR, J.W. & HASTIE, R.J. 1975 Relativistic limitations on runaway electrons. *Nuclear Fusion* **15** (3), 415.
- DECKER, J. & PEYSSON, Y. 2004 DKE: A fast numerical solver for the 3-D relativistic bounce-averaged electron drift kinetic equation. Technical report EUR-CEA-FC-1736. Plasma science and fusion center, MIT.
- DREICER, H. 1959 Electron and ion runaway in a fully ionized gas. I. *Phys. Rev.* **115**, 238–249.
- DREICER, H. 1960 Electron and ion runaway in a fully ionized gas. II. *Phys. Rev.* **117**, 329–342.
- ESPOSITO, B., MARTÍN-SOLÍS, J. R., POLI, F. M., MIER, J. A., SÁNCHEZ, R. & PANACCIONE, L. 2003 Dynamics of high energy runaway electrons in the Frascati Tokamak Upgrade. *Physics of Plasmas* (1994-present) **10** (6).
- FREDRICKSON, E.D., BELL, M.G., TAYLOR, G. & MEDLEY, S.S. 2015 Control of disruption-generated runaway plasmas in TFTR. *Nuclear Fusion* **55** (1), 013006.
- GILL, R.D., ALPER, B., DE BAAR, M., HENDER, T.C., JOHNSON, M.F., RICCARDO, V. &

- CONTRIBUTORS TO THE EFDA-JET WORKPROGRAMME 2002 Behaviour of disruption generated runaways in JET. *Nuclear Fusion* **42** (8), 1039.
- GILL, R. D., ALPER, B., EDWARDS, A. W., INGESSON, L. C., JOHNSON, M. F. & WARD, D. J. 2000 Direct observations of runaway electrons during disruptions in the JET tokamak. *Nuclear Fusion* **40** (2), 163.
- HAVLÍČEK, J. & HRONOVÁ, O. 2008 Characterization of magnetic fields in the COMPASS tokamak. In *WDS'08 Proceedings of Contributed Papers*. Prague, Czech Republic: Charles University.
- HAVLÍČEK, J. & HRONOVÁ, O. 2010 Magnetic diagnostics of COMPASS tokamak: <http://www.ipp.cas.cz/tokamak/euratom/index.php/en/compass-diagnostics/magnetic-diagnostics>.
- HENDER, T.C., WESLEY, J.C., BIALEK, J., BONDESON, A., BOOZER, A.H., BUTTERY, R.J., GAROFALO, A., GOODMAN, T.P., GRANETZ, R.S., GRIBOV, Y., GRUBER, O., GRYAZNEVICH, M., GIRUZZI, G., GINTER, S., HAYASHI, N., HELANDER, P., HEGNA, C.C., HOWELL, D.F., HUMPHREYS, D.A., HUYSMANS, G.T.A., HYATT, A.W., ISAYAMA, A., JARDIN, S.C., KAWANO, Y., KELLMAN, A., KESSEL, C., KOSLOWSKI, H.R., HAYE, R.J. LA, LAZZARO, E., LIU, Y.Q., LUKASH, V., MANICKAM, J., MEDVEDEV, S., MERTENS, V., MIRNOV, S.V., NAKAMURA, Y., NAVRATIL, G., OKABAYASHI, M., OZEKI, T., PACCAGNELLA, R., PAUTASSO, G., PORCELLI, F., PUSTOVITOV, V.D., RICCARDO, V., SATO, M., SAUTER, O., SCHAFER, M.J., SHIMADA, M., SONATO, P., STRAIT, E.J., SUGIHARA, M., TAKECHI, M., TURNBULL, A.D., WESTERHOF, E., WHYTE, D.G., YOSHINO, R., ZOHN, H., THE ITPA MHD, DISRUPTION & GROUP, MAGNETIC CONTROL TOPICAL 2007 Chapter 3: MHD stability, operational limits and disruptions. *Nuclear Fusion* **47** (6), S128.
- HOLLMANN, E. M., AUSTIN, M. E., BOEDO, J. A., BROOKS, N. H., COMMAUX, N., EIDIETIS, N. W., HUMPHREYS, D. A., IZZO, V. A., JAMES, A. N., JERNIGAN, T. C., LOARTE, A., MARTÍN-SOLÍS, J. R., MOYER, R. A., OOBURGOS, J. M. MU PARKS, P.B., RUDAKOV, D.L., STRAIT, E. J., TSUI, C., ZEELAND, M. A. VAN, WESLEY, J. C. & YU, J. H. 2013 Control and dissipation of runaway electron beams created during rapid shutdown experiments in DIII-D. *Nuclear Fusion* **53** (8), 083004.
- JANKY, F., HAVLÍČEK, J., BATISTA, A.J.N., KUDLACEK, O., SEIDL, J., NETO, A.C., PIPEK, J., HRON, M., MIKULIN, O., DUARTE, A.S., CARVALHO, B.B., STOCKEL, J. & PANEK, R. 2014 Upgrade of the COMPASS tokamak real-time control system. *Fusion Engineering and Design* **89** (3), 186 – 194, Design and implementation of real-time systems for magnetic confined fusion devices.
- LOARTE, A., RICCARDO, V., MARTÍN-SOLÍS, J.R., PALEY, J., HUBER, A., LEHNEN, M. & CONTRIBUTORS, JET EFDA 2011 Magnetic energy flows during the current quench and termination of disruptions with runaway current plateau formation in JET and implications for ITER. *Nuclear Fusion* **51** (7), 073004.
- MARTIN, G., CHATELIER, M. & DOLOC, C. 1995 New insight into runaway electrons production and confinement. In *22nd EPS Conference on Plasma Physics*. Bournemouth, United Kingdom: Plasma Physics and Controlled Fusion.
- MARTÍN-SOLÍS, J. R., LOARTE, A., HOLLMANN, E. M., ESPOSITO, B., RICCARDO, V., FTU, TEAMS, DIII-D & CONTRIBUTORS, JET EFDA 2014 Inter-machine comparison of the termination phase and energy conversion in tokamak disruptions with runaway current plateau formation and implications for ITER. *Nuclear Fusion* **54** (8), 083027.
- MARTÍN-SOLÍS, J. R., SÁNCHEZ, R. & ESPOSITO, B. 2010 Experimental observation of increased threshold electric field for runaway generation due to synchrotron radiation losses in the FTU tokamak. *Phys. Rev. Lett.* **105**, 185002.
- NILSSON, E., DECKER, J., PEYSSON, Y., GRANETZ, R.S., SAINT-LAURENT, F. & VLAINIĆ, M. 2015 Kinetic modelling of runaway electron avalanches in tokamak plasmas. *Plasma Physics and Controlled Fusion* Status: To Be Submitted.
- PÁNEK, R., BILYKOVÁ, O., FUCHS, V., HRON, M., CHRÁSKA, P., PAVLO, P., STÖCKEL, J., URBAN, J., WEINZETTL, V., ZAJAC, J. & ŽÁČEK, F. 2006 Reinstallation of the COMPASS-D tokamak in IPP ASCR. *Czechoslovak Journal of Physics* **56** (2), B125–B137.
- PAPŘOK, R., KRLÍN, L. & STÖCKEL, J. 2013 Observation and prediction of runaway electrons in the COMPASS tokamak. In *WDS'13 Proceedings of Contributed Papers*. Prague, Czech Republic: Charles University.

- REUX, C., PLYUSNIN, V., ALPER, B., ALVES, D., BAZYLEV, B., BELONOHY, E., BREZINSEK, S., DECKER, J., DEVAUX, S., DE VRIES, P., FIL, A., GERASIMOV, S., LUPELLI, I., JACHMICH, S., KHILKEVITCH, E.M., KIPTILY, V., KOSLOWSKI, R., KRUEZI, U., LEHNEN, M., MANZANARES, A., MLYNÁŘ, J., NARDON, E., NILSSON, E., RICCARDO, V., SAINT-LAURENT, F., SHEVELEV, A.E., SOZZI, C. & CONTRIBUTORS, JET EFDA 2014 Runaway beam studies during disruptions at JET-ILW. In *21st International Conference on Plasma Surface Interactions*. Kanazawa, Japan: Journal of Nuclear Materials.
- ROSENBLUTH, M.N. & PUTVINSKI, S.V. 1997 Theory for avalanche of runaway electrons in tokamaks. *Nuclear Fusion* **37** (10), 1355.
- SAINT-LAURENT, F., BUCALOSSI, J., REUX, C., BREMOND, S., DOUAI, D., GIL, C. & MOREAU, P. 2011 Control of runaway electron beam heat loads on Tore Supra. In *38th EPS Conference on Plasma Physics*. Strasbourg, France: Plasma Physics and Controlled Fusion.
- SAINT-LAURENT, F., REUX, C., BUCALOSSI, J., LOARTE, A., BREMOND, S., GIL, C. & MOREAU, P. 2009 Control of runaway electron beams on Tore Supra. In *36th EPS Conference on Plasma Physics*. Sofia, Bulgaria: Plasma Physics and Controlled Fusion.
- SMITH, H. M. & VERWICHTE, E. 2008 Hot tail runaway electron generation in tokamak disruptions. *Physics of Plasmas (1994-present)* **15** (7), 072502.
- VLAINIĆ, M., MLYNÁŘ, J., WEINZETTL, V., PAPŘOK, R., IMRÍSEK, M., FICKER, O., VONDŘÁČEK, P. & HAVLÍČEK, J. 2014 First dedicated observations of runaway electrons in COMPASS tokamak. *Nukleonika* Status: Submitted For Publication.
- YOSHINO, R., TOKUDA, S. & KAWANO, Y. 1999 Generation and termination of runaway electrons at major disruptions in JT-60U. *Nuclear Fusion* **39** (2), 151.
- YU, J. H., HOLLMANN, E. M., COMMAUX, N., EIDIETIS, N. W., HUMPHREYS, D. A., JAMES, A. N., JERNIGAN, T. C. & MOYER, R. A. 2013 Visible imaging and spectroscopy of disruption runaway electrons in DIII-D. *Physics of Plasmas (1994-present)* **20** (4), 042113.